

Lawrence Berkeley National Laboratory

Lawrence Berkeley National Laboratory

Title

PHYSICAL CHANGES IN THE PORE STRUCTURE OF COAL WITH CHEMICAL PROCESSING

Permalink

<https://escholarship.org/uc/item/1dt494d8>

Author

Harris Jr, E.C.

Publication Date

1978-03-01

0 0 0 0 4 9 0 2 1 7 5

UC-90a

LBL-6891

C.1

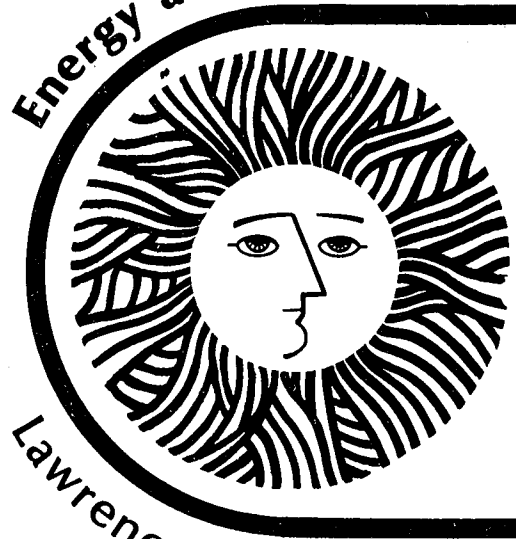
RECEIVED
LAWRENCE
BERKELEY LABORATORY

JUN 14 1978

LIBRARY AND
DOCUMENTS SECTION

For Reference
Not to be taken from this room

Energy and Environment Division



Physical Changes in the Pore Structure
of Coal with Chemical Processing

Everette C. Harris, Jr.
(M. S. Thesis)

March 1978

Lawrence Berkeley Laboratory University of California/Berkeley

Prepared for the U.S. Department of Energy under Contract No. W-7405-ENG-48

90

LBL-6891
C.1

LEGAL NOTICE

This report was prepared as an account of work sponsored by the United States Government. Neither the United States nor the Department of Energy, nor any of their employees, nor any of their contractors, subcontractors, or their employees, makes any warranty, express or implied, or assumes any legal liability or responsibility for the accuracy, completeness or usefulness of any information, apparatus, product or process disclosed, or represents that its use would not infringe privately owned rights.

PHYSICAL CHANGES IN THE PORE STRUCTURE OF COAL WITH CHEMICAL PROCESSING

Contents

Abstract	v
I. Introduction	1
A. Pore Structure of Coal	1
B. Measurement of Coal Surface Area	4
C. Measurement of Pore Volumes and Distributions	8
D. Chemical Processing of Coal	10
E. Objectives	11
References	12
II. Equipment and Procedures	14
A. Adsorption and Actual-Density Apparatus	14
B. Degassing, Adsorption, Helium Displacement and Calculated Procedures	16
C. Porosimeter	20
D. Porosimeter Procedures and Calculations	20
References	23
III. Properties of Raw Roland Seam Coal	24
A. Introduction	24
B. Preparation and Storage	24
C. Chemical Analysis	25
D. Physical Analysis	25
References	29

IV. Physical Properties of Extracted Coals	30
A. Introduction	30
B. Extracted Coal Samples	30
C. Surface Areas of the Extracted Coals	32
D. Pore Volumes and Distributions	37
References	44
V. Surface Area Variation of Reacted Roland Seam Coal	45
References	45
VI. Conclusions and Suggestions for Future Work	48
A. Conclusions	48
B. Suggestions	49
References	49
Acknowledgement	50
Appendix A. A Method of Determining Particle Densities of Spheroids	51
References	53

PHYSICAL CHANGES IN THE PORE STRUCTURE OF COAL WITH CHEMICAL PROCESSING

Everette C. Harris, Jr.

Energy and Environment Division, Lawrence Berkeley Laboratory
and Chemical Engineering Department, University of California,
Berkeley, California 94720

Abstract

The physical structure of Roland Seam coal was characterized by studying the surface areas, pore volumes, and pore distributions of raw coal, extracted coals, and reacted coals. BET surface areas were measured by carbon dioxide adsorption at 195°K and nitrogen adsorption at 77°K. Pore volumes were calculated by the difference in the reciprocals of measured apparent and actual densities. Distribution curves were generated by measuring mercury penetration as a function of pressure.

The data gathered suggests a micropore structure having a 34 Å average diameter and random constrictions of the order of 4 Å. Extraction generates new micropores and degrades the micropore structure, for yields in excess of 35% occur. Changes in the pore distribution and the generation of new pores indicate that resistance to extraction due to the pore structure is minimal, while pore-volume data confirm the preferential liquefaction of lower-molecular-weight material. Increases in surface roughness due to pretreatment of the coal indicate a higher selectivity of solvents after hydrogenation of the coal. A study of the BET constant implies that the surface becomes more favorable to carbon dioxide adsorption with increasing extraction.



I. INTRODUCTION

Coal has a highly complex internal pore system similar in many ways to molecular sieves. In order for chemical reactions, gas adsorptions, and extractions to take place, reagents or vapors have to pass into the micropore structure of coal. Rates of mass transfer may be greatly restricted by the very small size of the openings in the coal structure.

The internal structure of coal should be maintained during processing to allow the processing fluid to be in contact with as much of the solid coal as possible. Therefore the pore volume and surface area should be measured as processing takes place, to determine if the internal structure of coal is being utilized effectively. If not, the processing variables should be modified to achieve this whenever possible.

To follow the changes in the pore structure of coal during chemical processing, reliable experimental methods are needed to measure the internal structure. The surface area, pore volume, and apparent and actual densities are fundamental properties of porous solids. Because the solid surface of coal is the place where key physical and chemical phenomena occur, knowledge of changes in the pore system should provide insight into the mechanisms of the chemical processing of coal.

A. Pore Structure of Coal

Van Krevelen and Zwietering (1) first applied Riter and Drake's (2) method of mercury penetration to the study of coal. This work suggests that coal contains two pore systems (1) a macropore

system and (2) a micropore system. Generally pores in the size range below 12 A are described as micropores, those above 200 A as macropores, and the in between as transitional or intermediate pores. Mercury is able to penetrate the macropore system but even at high pressures it is unable to penetrate the micropore system. However, both pore systems are accessible to helium at room temperature.

The pore size distribution can vary greatly depending on the rank of coal. Gan, Nandi, and Walker (3) measured the pore size distributions for a number of coals by nitrogen adsorption isotherms at 77°K. They determined the cumulative pore volume, in the pore range of 30000 A to 12 A. For an Illinois No. 6 high-volatile-C bituminous coal, 30.2% of the pore volume is smaller than about 12 A, 52.6% between 12 A and 300 A, and 17.2% above 300 A. For a low volatile bituminous Pennsylvania coal, 73% of the pore volume is under 12 A, 0% between 12 A and 300 A, and 27% above 300 A.

Medeiros and Petersen (4) have recast Walker's results as shown below. The surface area distribution for the Illinois No. 6 coal then becomes

<u>Pore Size</u>	<u>Surface Area</u>	<u>Pore Volume</u>
less than 12 A	156 m ² /g	0.039 cc
12-300 A	26 m ² /g	0.065 cc
greater than 300 A	1 m ² /g	0.026 cc

The above surface-area breakdown show that most of the internal surface area of coal is contained in the micropores.

As already mentioned, the internal structure of coal has certain characteristics of molecular sieves. Bond and Spencer (5) observed that the heat of wetting for any rank of coal decreases as the molecular volume of the wetting liquid increases. They obtained a relationship for the ultrafine internal surface area as a function of size, showing that the critical dimensions of ultrafine pores are 5 A and 8 A in approximate diameters, corresponding to molecular diameters of wetting liquids whose molecular volumes are around 50 and 150 cc/mole.

Lamond and Marsh (6) and later Medeiros and Petersen used 4 A and 5 A molecular sieves to study the pore diameters of coal. Marsh observed that nitrogen at 77°K would penetrate 5 A sieves but not 4 A sieves, whereas carbon dioxide at 195°K had no difficulty penetrating either.

Medeiros made further use of the molecular sieve properties of coal to determine a rough pore size distribution. He used the adsorption of four gases (CO₂, CF₄, N₂, and Ar) on Wyodak Roland coal, Illinois No. 6 coal, and 4 A and 5 A Linde molecular sieves to study the microporous structure of coal. The reasoning was that the penetration depended upon the size of the adsorbate. Medeiros concluded that Roland Seam coal resembles a 4 A sieve in its micropore structure, whereas the Illinois No. 6 coal more closely resembles the 5 A molecular sieve.

Booras and Petersen (7) studied high and low temperature adsorption of CO₂ on an alumina catalyst, a synthetic sodium mordenite, and Roland Seam coal. They used 195°K and room temperature, and concluded that activated diffusion was not an important factor in adsorption at either

of these temperatures, for samples having pore diameters as low as 6.7 Å.

B. Measurement of Coal Surface Area

The determination of the surface area of coal is not straightforward. No method has so far been described which can be applied to all coals without some degree of criticism.

The method of heat of wetting has been in use for many years and is based on a measurement of the amount of heat liberated when the internal surface is completely wetted by either methanol or water. Griffith and Hirst (8) and Maggs (9) initially determined the total internal surface area of coal by this method. This method suffers from two main disadvantages. First it is necessary to have a conversion factor to obtain units of area from units of energy. This factor is only constant if one assumes that all coals have energetically similar surfaces. Secondly, some of the heat liberated is actually due to solution rather than adsorption. Using a conversion factor of 400 ergs/cm², Bond and Maggs (10) found surface areas of coal between 20 and 200 m²/g depending on the rank of coal.

The best known method for determining the specific surface area of porous solids is obtained from the work of Brunauer, Emmitt, and Teller (BET) (11-13). The method is based on the determination of the number of molecules of gas which, when adsorbed on the surface of a solid, completely cover the solid with a monolayer of the gas. This value multiplied by the cross-sectional area per molecule gives directly the surface area. The BET method involves measuring the adsorption isotherms of gases near their condensation pressure. The

required data may be obtained by either volumetric or gravimetric measurements.

The specific surface area, S , in square meters per gram is given by:

$$S = (V_m A_m N / (V_0 W)) \times 10^{-20}$$

where:

V_m = the gas uptake for a monolayer coverage corrected to STP, cc.

N = Avogadro's number (6.023×10^{23}), molecules per mole.

V_0 = the ideal gas volume per mole (22414 cc/mole) at STP.

W = the mass of the sample in grams.

A_m = the average area occupied by the adsorbed gas molecule in angstroms squared per molecule of adsorbate.

V_m is obtained by determining the volume of gas adsorbed (referred to STP) at a number of equilibrium relative pressures by use of the BET equation:

$$\frac{P_2}{V_a(P_0 - P_2)} = \frac{1}{V_m C} + \frac{(C - 1) P_2}{V_m C P_0}$$

where:

V_a = the volume of gas adsorbed referred to STP

P_2 = the equilibrium pressure of the adsorbate

P_0 = the vapor pressure of the adsorbate at the temperature of adsorption

C = the BET constant, related to the relative rates of adsorption of the first and second layers of adsorbate. It is given as:

$$C = \frac{a_1 b_2}{a_2 b_1} \exp(E_1 - E_L)/RT$$

where:

E_1 = the heat of adsorption in the first layer

E_L = the heat of liquefaction of the adsorbate

R = the gas constant

T = the adsorbate temperature

The pre-exponential coefficient is generally considered unity.

A plot of $P_2/(V_a(P_0 - P_2))$ vs P_2/P_0 gives a straight line with an intercept of $1/(V_m C)$ and a slope of $(C - 1)/(V_m C)$. From the plot C and V_m are calculated. At least four points with relative pressures in the range of 0.05-0.30 are usually utilized.

Average molecular areas were obtained by Medeiros, in calibration runs on two Harshaw catalyst using nitrogen at 77°K. For nitrogen, $A_m = 16.2 \text{ A}^2$. For all other gases, A_m values were chosen such that the calculated areas were the same as the nitrogen surface areas. Values of 17.0, 23.4, and 17.3 A^2 were obtained for the argon, carbon dioxide, and carbon tetrafluoride molecules respectively.

Maggs (14-16) showed that the equilibrium amount of nitrogen adsorbed on coal reaches a maximum at 195°K. Below this temperature the rate of adsorption is very low and equilibrium is not reached in any reasonable length of time. Booras confirmed that the low temperature nitrogen BET surface areas of coal are very small. Maggs concluded that either some temperature-dependent physical changes in the structure such as thermal contraction of the pores was occurring, or the diffusion of nitrogen into very fine pores of coal is an activated

process whereby the rate of diffusion into the micropores would not become sufficiently rapid until above about 100°K.

Zwietering and Van Krevelen (17) measured the density of coal in helium over a temperature range from 77°K to 373°K and observed no contraction of the internal volume of the coal. It appears that the contraction of the internal volume of the coal. It appears that temperatures are a result of the inability of the molecules to diffuse into the ultrafine pore structure of coal, rather than to the thermal contraction of coal.

The adsorption of rare gases on coal also has been measured. Lahiri et al. (18) studied the adsorption of argon at 0°C on several coals and cokes. Lahiri obtained BET surface areas ranging from 13 to 51 m²/g for a British anthracite coal. Kini (19) obtained surface areas from 140 to 200 m²/g, depending on the coal studied.

Carbon dioxide has been used extensively in recent years to measure the internal surface areas of coal. Anderson et al. (20) obtained surface areas for a low volatile bituminous Pittsburgh coal of 114 and 140 m²/g from carbon dioxide adsorption at 195°K. Walker and Geller (21) also used carbon dioxide to obtain an area of 175 m²/g for an anthracite coal. Czerski, Korla, and Lason (22) compared surfaces areas calculated by carbon dioxide adsorption and by the heat of wetting method for several different coals. The carbon dioxide areas were lower than the heat of wetting values for all samples.

Lamond, Marsh, and Wynne-Jones (6,23) studied the adsorption of carbon dioxide on many carbonaceous materials. They concluded that carbon dioxide can be used satisfactorily at 195°K as an absorbate

to determine surface areas of coal. Anderson (20) stated the true value of the total surface area of coal probably lies between the value obtained from CO₂ adsorption at 195°K and the heat of wetting values using methanol.

Walker and Nandi (3) compared carbon dioxide adsorption at 195°K and nitrogen adsorption at 77°K on several types of coal. On all of their samples, the areas obtained using nitrogen were always lower than those obtained using carbon dioxide. For some coals the nitrogen surface areas were less than 1 m²/g, while for other coal samples the nitrogen surface area was as high as 90 m²/g.

C. Measurement of Pore Volumes and Distributions

Three of the most commonly used methods of experimentally determining pore volumes are by reciprocal densities (24), capillary condensation (25), and moisture content (26). Each of these procedures has some disadvantage.

The method of reciprocal densities requires two independent experiments. One is the determination of a real density. The other is the determination of an apparent density. The real density is easily measured by helium displacement (17), where it is assumed that helium penetrates all of the pores of the specimen. The apparent density is found by mercury penetration. For porous solids having large amounts of macropores, one must judiciously determine when interparticle voids are filled and when pores are being filled. Choosing a narrow-sample size distribution reduces this problem immensely. The advantage of this procedure is that the macropore distribution can be determined by increasing the mercury intrusion.

Assuming the Washburn Eq. (27) is valid and knowing the equilibrium penetration as a function of pressure, one can obtain the pore distribution. Since mercury will not penetrate micropores, this procedure is valid only for the macropores. The Washburn equation is:

$$p = - \frac{2\sigma \cos \alpha}{r}$$

where

p = total pressure

σ = surface tension

α = wetting angle

r = pore radius

The capillary condensation method requires one to assume either Wheeler's composite of the BET multilayer adsorption theory (28) or the Kelvin Eq. (28). These describe the pore distribution by determining the pressures up to the condensation pressure of the gas. This technique almost invariably yields pore volumes that are too large, because at high pressures the theory of capillary condensation predicts pore openings larger than they actually are (29).

The method of moisture content requires that the actual density of coal be known, and assumes that all pores are filled with water by boiling the sample in water (26). After drying and recording the weight loss, one obtains the pore volume from the density of water. The principle disadvantage of this method is that it tells nothing about the pore distribution and yields pore volumes which are too low because of entrapped gases.

Walker (3) obtained complete pore size distributions by mapping the mercury intrusion (macropore distribution) and the capillary condensation (micropore distribution) together. He was able to get an accurate distribution over the full range of radii.

D. Chemical Processing of Coal

New chemical processes must be developed in order to make full use of our vast resources of coal to help supply our increasing need for energy and hydrocarbons. Coal research in the Department of Chemical Engineering at the University of California, Berkeley is proceeding along several lines. These include production of liquid hydrocarbons by solvent extraction and zinc chloride hydrogenation.

There are four general conceptual approaches to converting coal to liquid products. These are: The production of H_2/CO mixtures from coal followed by a catalytic synthesis of higher hydrocarbons from this gas, partial dissolution with solvents without significant hydrogenation, partial dissolution with hydrogenation by a solvent, and staged pyrolysis.

There has been much research recently on the production of liquid products from coal at sub-pyrolysis temperatures. The changes in the pore structure of coal due to extraction by several organic solvents independently, with and without catalytic hydrogenation, are examined here.

A better understanding of the internal structure of coal would be very helpful in studying the action of prospective coal solvents. A knowledge of the chemical and physical processes involved may suggest new or improved processes.

E. Objectives

The objective of this research was to characterize the internal structure of raw coal and to follow the changes in the pore volume, actual density, apparent density, macropore distribution, and surface areas. Reliable methods were developed to measure each of these. An attempt to determine the shape of micropores is made using the above data.

REFERENCES

- (1) P. Swietering and D. W. Van Krevelen, *Fuel* 33, 331 (1954).
- (2) H. L. Ritter and L. C. Drake, *Ind. Eng. Chem.* 17, 780 (1949).
- (3) H. Gan, S. P. Nandi and P. L. Walker, *Fuel* 51, 272 (1972).
- (4) D. Medeiros and E. E. Petersen, Lawrence Berkeley Laboratory Report LBL-4439 (1975).
- (5) R. L. Bond and D. Spencer, *Ind. Carbon and Graphite*, 231 (1958).
- (6) T. G. Lamond and H. Marsh, *Carbon* 1, 281 (1964).
- (7) G. S. Booras and E. E. Petersen, Lawrence Berkeley Laboratory Report LBL-5272 (1976).
- (8) M. Griffith and W. Hirst, Proceedings of the Conference of the Ultrafine Structure of Coal and Coke, BCRUA, 80 (1943).
- (9) F. P. A. Maggs, Proceedings of the Conference of the Ultrafine Structure of Coal and Coke, BCRUA, 95 (1943).
- (10) R. L. Bond and F. P. A. Maggs, *Fuel* 28, 172 (1949).
- (11) S. Brunauer, P. Emmett and E. Teller, *J. Am. Chem. Soc.* 60, 309 (1938).
- (12) P. Emmett and S. Brunauer, *J. Am. Chem. Soc.* 59, 1553 (1937).
- (13) S. Brunauer, W. E. Deming and E. Teller, *J. Am. Chem. Soc.* 62, 1723 (1940).
- (14) F. P. A. Maggs, *Nature* 169, 793 (1952).
- (15) F. P. A. Maggs and I. Dryden, *Nature* 169, 269 (1952).
- (16) F. P. A. Maggs, *Research*, Vol. IV, No. 2, D1 (1952).
- (17) P. Zwietering and D. W. Van Krevelen, *Fuel* 33, 331 (1954).
- (18) K. A. Kini, S. P. Nandi, J. N. Sharma, M. S. Iyengar and A. Lahiri, *Fuel* 35, 71 (1956).

- (19) K. A. Kini, Fuel 43, 173 (1964).
- (20) R. B. Anderson, L. J. E. Hofer and J. Bayer, Fuel 41, 559 (1962).
- (21) P. L. Walker and I. Geller, Nature 178, 1001 (1956).
- (22) L. Czerski, A. Korta, and M. Lason, Roczn. Chem. 31, 227 (1957).
- (23) H. Marsh and W. F. K. Wynne-Jones, Carbon 1, 269 (1964).
- (24) Y. Toda, Fuel 52, 36 (1953).
- (25) E. Barrett, L. G. Joyner and P. P. Halenda, J. Am. Chem. Soc. 73, 373 (1951).
- (26) J. Thomas and H. Damberger, Illinois State Geological Survey, Circular 493 (1975).
- (27) E. Washburn, Proc. Natl. Acad. Sci. 7, 115 (1921).
- (28) A. Wheeler, AAAS Gordon Conference on Catalysis Report No. S-9829 (1945).
- (29) C. G. Shull, J. Amer. Chem. Soc. 70, 1405 (1948).

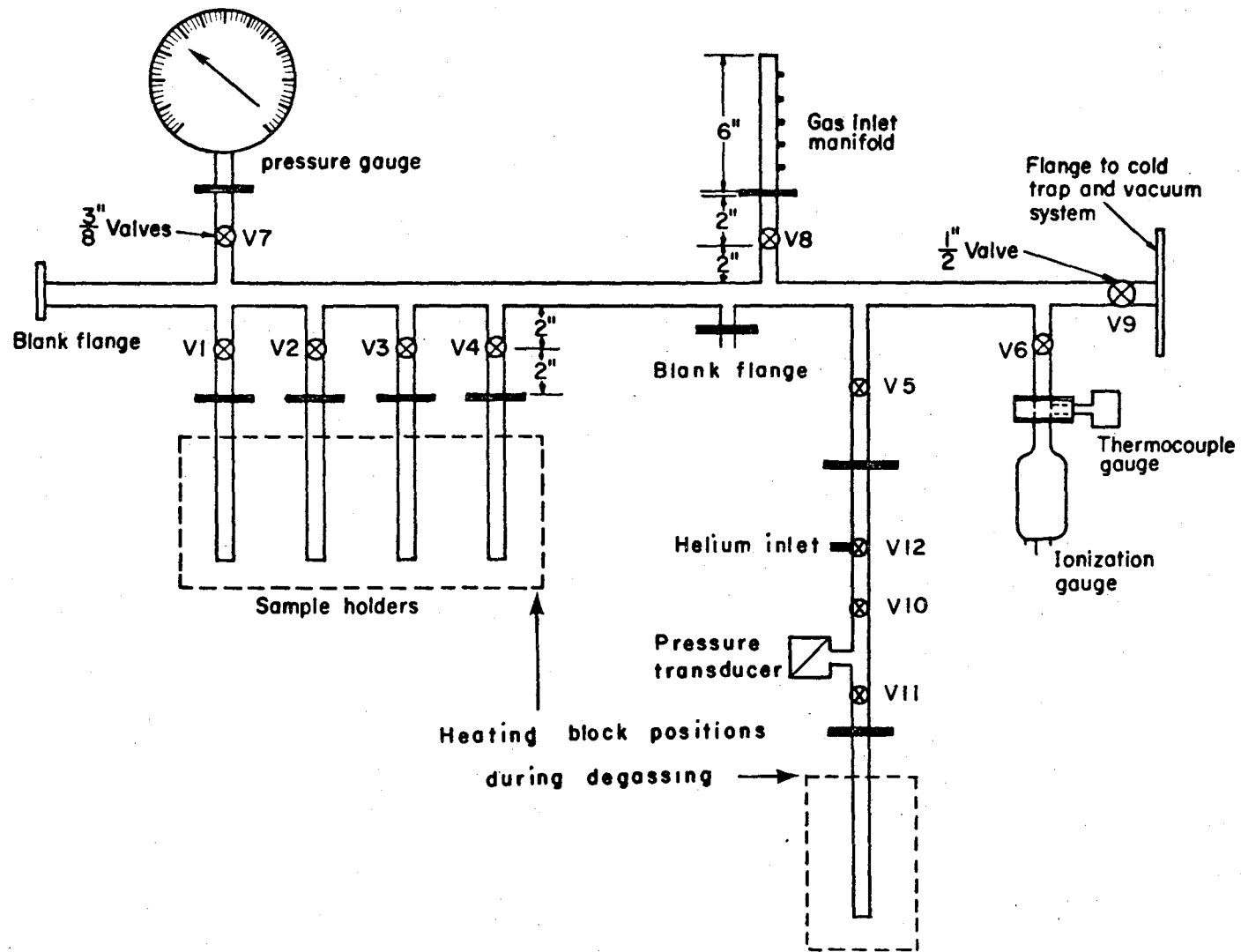
II. EQUIPMENT AND PROCEDURES

A. Adsorption and Actual-Density Apparatus

The adsorption apparatus used in this research was designed and constructed by Medeiros and Petersen (1), who have described the equipment in detail. The apparatus has two interchangeable manifolds to permit a high-pressure or a low-pressure determination of the surface area of porous materials. Although the wall thickness of the 304 stainless steel tubing used is different in the two manifolds, the linear dimensions are identical. The system, capable of handling up to five samples simultaneously, is shown in Fig. II-1. The low pressure manifold was used exclusively in this study.

For degassing, the samples are heated with a temperature controlled aluminum heating block. Vacuum is produced by an oil diffusion pump in series with a mechanical vacuum pump. The degassing pressure read by ionization and thermocouple gauges. Three interchangeable pressure gauges (0-800 mm Hg, 0-80 psig, and 0-800 psig) are used to read the manifold pressure.

The helium-density apparatus is attached to the flange below valve V5, so as to allow simultaneous helium-density and surface area measurements. by the authors. With reference to Fig. II-1, valves V10, V11, and V12 are 1/8 in. Hoke valves, Model No. 4171M2B. The pressure transducer is a Calvin Labs. Inc. 0-50 psia, Model No. 40121-A05-100. The 0-80 psig gauge was used to calibrate the pressure transducer output voltage, which was read on a Fairchild Model No. 320759 digital voltmeter. A Mallory Model No. 303369 mercury



000004902105

XBL 784-560

Fig. II-1. Assembled adsorption manifold.

battery was used as a power source. A Brisket temperature controller Model No. TS94-5 was used to control the degassing temperature.

The volume of the sample holder 5 was calibrated by repeated water displacement measurements at different temperatures. The reference volume, which is enclosed by V10 and V11, was calibrated by the method of Medieros and Petersen. The resulting volumes are 3.414 cc and 5.077 cc for the sample holder and reference volumes respectively.

B. Degassing, Adsorption, Helium Displacement and Calculated Procedures

Empty sample holders with the spacers inserted were weighed to within 0.0001 grams on a microbalance. The samples were then placed into the sample holders, and the loaded sample holder assemblies were weighed. The weights of the samples were found by difference.

Valves V1 to V7 and V9 to V11 were opened while valves V8 and V12 remained closed during degassing. The vacuum pump was then turned on to evacuate the system. The heating blocks were raised into position and the temperature controllers were turned on. Coal samples were degassed at 130°C for about 16 hr. After the pressure fell below 0.1 torr, the diffusion pump and cooling water were turned on. Liquid nitrogen was poured into the cold trap to condense any oil vapors and prevent them from entering the system. After the samples were degassed for approximately 16 hr at a pressure near 10^{-5} torr, the temperature controllers were turned off, and the heating blocks were lower and removed. Sample holders 1 and 2 were placed in a dry ice/acetone bath, followed by a 30 min cooling down period for the sample holders to achieve thermal equilibrium (1 and 2 to dry ice temperature, 3, 4, and 5 to room temperature). All valves were then closed and

the diffusion pump was turned off. The cooling water and vacuum pump were turned after or additional 30 min, when the diffusion pump oil had cooled.

Valves V11, V10, and V12 were opened, and helium was admitted to the helium system until a pressure of about 1700 torr absolute pressure was reached. Valve V12 and V10 were then closed. Two hours were allotted for the helium to achieve equilibrium, the time that it took to do the adsorption of sample holder 1. Valve V11 was then closed and the sample holder pressure (P_{sh}) was recorded. With valves V5, V6, V9 and V10 open the system was pumped down to less than 100 microns. Valves V5, V6, V9, and V10 were then shut, and V11 was opened. The helium was again allowed 2 hr to equilibrate as the adsorption experiment of sample holder 2 was being done. At this time, V11 was closed and the final pressure (P_f) was recorded.

The adsorption procedure was the same as that used by Medeiros and Petersen. The adsorbate gas was admitted into the manifold through V8 while valves V1 to V4, V6, V9 and V10 were closed. Then valves V5 and V8 were closed and the manifold pressure and temperature was recorded. Valve V1 was then opened to allow the gas to expand into the sample holder and be adsorbed. An equilibration time of 30 min was allowed before the final pressure and temperature were recorded. The sample holder valve was then closed and the procedure as repeated at a higher initial pressure. Four adsorption points in the pressure range of 0.05 to 0.30 atmospheres were taken for each sample. After the four pairs of data were taken, valve V1 was closed and V5, V6, V9 and V10 were opened and the manifold was evacuated to less than

100 microns. During the evacuation sample holder 1 was removed from the dry ice bath and sample holder 3 was placed in it. The procedure was repeated for sample holders 2-4.

The following equation for the volume of gas adsorbed at standard conditions was developed by Medeiros and Petersen:

$$V_i = \frac{T_s V_m}{P_s m} \left[\frac{P_{1,n}}{T_{1,n}} - \frac{P_{2,n}}{T_{2,n}} + \frac{V_{sh1}}{V_m} \left[\frac{P_{2,n-1}}{T_{2,n-1}} - \frac{P_{2,n}}{T_{2,n}} \right] \right. \\ \left. + \left[\frac{V_{sh2} - V_s}{V_m T_0} \right] (P_{2,n-1} - P_{2,n}) \right]$$

$$V = \sum_{i=1}^N V_i$$

where:

n = adsorption point indicator; 1,2,3,4,

m = weight of the porous solid less volatiles, grams,

$P_{1,n}$ = initial pressure in manifold before expanding the adsorbate into the sample holder for the n^{th} adsorption point,

$P_{2,n}$ = final pressure in the manifold after expanding the adsorbate gas into the sample holder for the n^{th} adsorption point,

when $n-1 = 0$, $P_{2,n-1} = 0$,

P_s = standard pressure, 760 torr,

$T_{1,n}$ = initial temperature of the manifold for the n^{th} point, $^{\circ}\text{K}$,

$T_{2,n}$ = final temperature of the manifold for the n^{th} point, $^{\circ}\text{K}$,

T_0 = adsorption temperature, $^{\circ}\text{K}$,

T_s = standard temperature, 273 $^{\circ}\text{K}$,

V_m = manifold volume, cc,

V_{sh} = sample holder volume, cc.

V_{sh1} = volume of sample holder not immersed in the liquid bath, cc.

This volume was considered to be at the same temperature as the manifold.

V_{sh2} = volume of the sample holder immersed in the liquid bath, cc. This volume was considered to be at temperature T_0 ,

V_s = volume of the porous solid, cc,

V_i = volume of gas adsorbed referred to STP per gram of sample during the n^{th} equilibration, cc/g,

V = total volume of gas adsorbed referred to STP per gram of sample, cc/g.

The value of V obtained from the equation was then used to construct a BET plot. The volume adsorbed for a monolayer on the surface, X_m , could then be calculated from the slope and intercept of the BET plot. The product of X_m and the cross sectional area per molecule, A_m , gives the total surface area per gram of porous solid sample. Values of A_m were obtained from the paper by Medieros and Petersen.

Actual densities were determined by:

$$\rho = \frac{m}{\left[V_{sh} + \left[\frac{P_f}{P_f - P_{sh}} \right] V_r \right]}$$

where:

m = mass of sample, grams.

V_{sh} = volume of empty sample holder, cc.

V_r = volume of reference volume, cc.

P_{sh} = initial pressure in sample holder, torr.

P_f = final pressure in system, torr.

ρ = helium density, g/cc.

C. Porosimeter

The porosimeter used in this study was an Aminco-Winslow Porosimeter Model No. 5-7118 (see Fig. II-2). It is a completely hydraulic apparatus capable of detecting pore volumes as small as 0.001 cc and pores having diameters of 0.035 microns or larger. Pressures up to 5000 psig are obtained by a hand operated fluid pump.

D. Porosimeter Procedures and Calculations

An empty penetrometer was weighed to within 0.0001 grams and then placed into the filling device. The system was then pumped down to less than 50 microns. After tilting the glass filling device, until the end of the penetrometer stem was immersed completely in mercury, the stopcock was opened to allow air to expand into the vacuum chamber until a pressure of 6.8 psia was obtained. Sufficient to completely fill the device. The stopcock was reopened to allow equilization of pressure with the atmosphere after the filling device was placed in the upright position. The filled empty penetrometer was weighed and carefully emptied into the filling device.

A small quantity of sample (about 0.2 grams), which had been degassed in a vacuum oven (105°C and 15 in. Hg vacuum) for 16 hr,

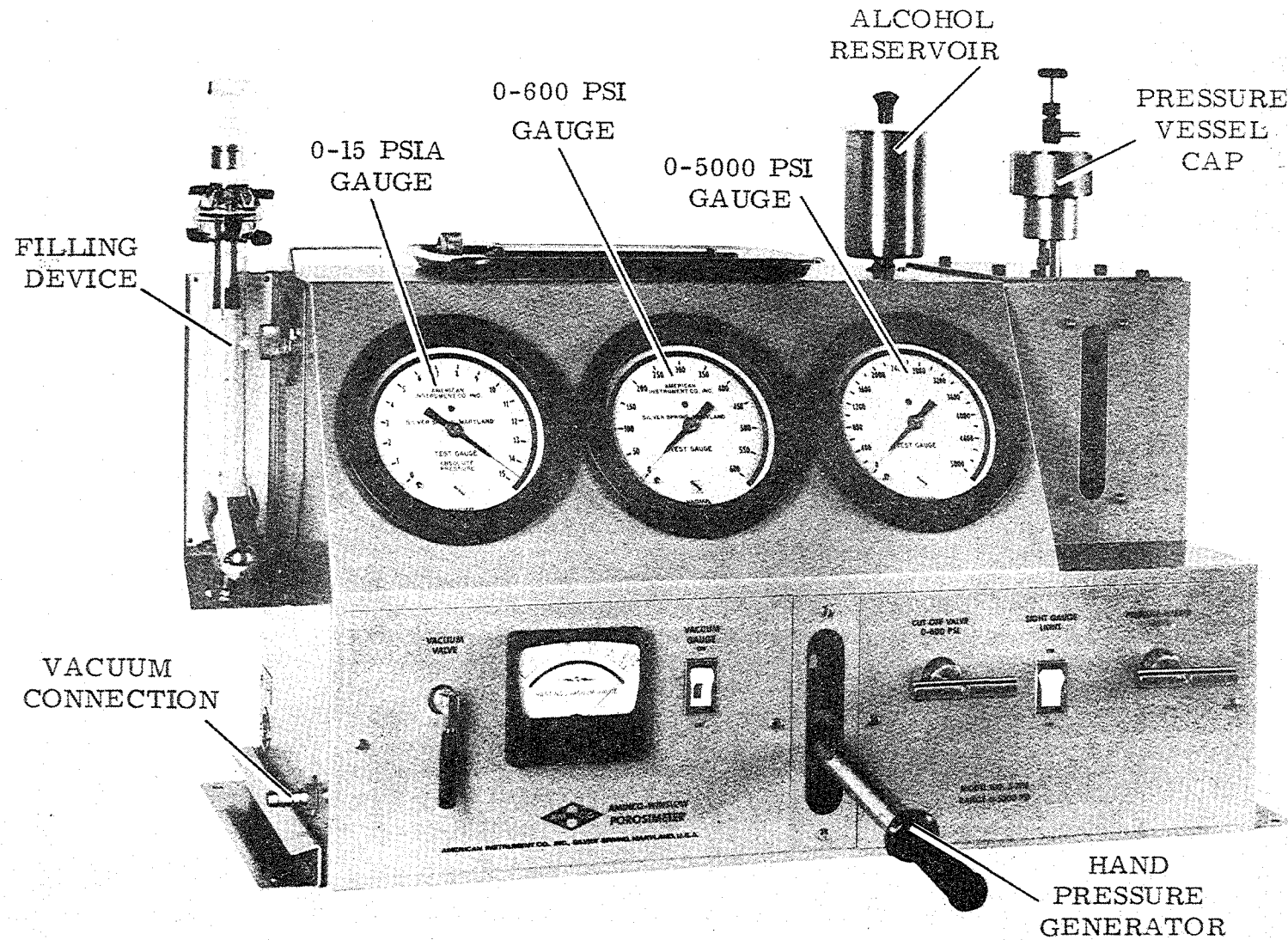


Fig. II-2. Aminco-Minslow porosimeter, model No. 5-7118.

XBB 783-2788

was placed into the empty penetrometer. The penetrometer with sample was then weighed, the weight of sample being obtained by difference. The filling procedure was repeated until a pressure of 6.8 psia is reached. About 10 min were allowed for equilibration before the stem was removed from the mercury.

Air was allowed to enter the filling device until desired pressures were obtained (about 9, 11, 13 and 14.7 psia). The pressure and their corresponding penetrometer stem readings were recorded. When atmospheric pressure was reached, the penetrometer was again removed and weighed.

The penetrometer was placed into the pressure vessel after the alcohol reservoir (filled with isopropyl alcohol) was raised. The bleeder valve and the cut off valve were opened after the pressure release valve was closed. By using the handpump, air was removed from the system the bleeder valve was then closed and the pressure increased, taking data as desired. Before reaching 600 psig, the cut off valve was closed. Readings up to 5000 psig were then taken. Due to the heat of compression the pressure must be allowed to stabilize before it is recorded.

Apparent densities were determined by:

$$\rho_a = (w_s \rho_{Hg}) / (w_e + w_s - w_f)$$

where:

w_s = the weight of sample, grams.

w_e = the weight of the empty penetrometer, grams.

w_f = weight of the penetrometer plus sample completely filled with mercury, grams.

ρ_{Hg} = density of mercury, grams/cc.

ρ_a = the apparent (particle) density, grams/cc.

Pore volumes are determined by:

$$V_p = 1/\rho_a - 1/\rho$$

where:

V_p = the pore volume, cc/grams.

Pore volume distribution curves were obtained by assuming cylindrical pores (Washburn equation applies) and plotting cumulative pore volume vs equivalent pore diameter. The cumulative pore volume is the volume of all pores whose diameter is smaller than the equivalent pore diameter.

REFERENCE

- (1) D. Medeiros and E. Petersen, Lawrence Berkeley Laboratory Report LBL-4439 (1975).

III. PROPERTIES OF RAW ROLAND SEAM COAL

A. Introduction

This highly aromatic material has a unique pore structure. The following experimental observations suggest that the micropore system has a random set of narrow constrictions: (1) surface area measurements by carbon dioxide and nitrogen are $99.3 \text{ m}^2/\text{g}$ and less than $1 \text{ m}^2/\text{g}$, respectively and (2) unlike carbon dioxide, nitrogen will not penetrate a 4 A molecular sieve (1). To test this model of the pore system, detailed pore volume studies were made to determine the average micropore diameter by assuming a cylindrical pore shape. If that micropore diameter is much larger than 4A, there must be a set of narrow constrictions of the order of 4 A in the pore system, in order to account for the above experimental observations.

B. Preparation and Storage

This subbituminous coal was obtained from the Roland top seam of the Wyodak Mines at Gillette, Wyoming. This coal was used in the studies of Grens et al. (2-4). The as-received coal was reduced to minus 1/32 in. following ASTM Method D-346. This minus 1/32 in. coal was separated by alternate shovels into 15 pound portions and sealed in plastic bags which were stored in a 55-gal drum. As needed, representative samples were taken from these bags using a riffler. These samples were further reduced in size in a ball mill to -28 + 150 Tyler mesh and subsequently placed in a desiccator under either vacuum or stored under nitrogen in friction-lid paint cans. This coal, -28 + 150 mesh, was used in this study and by Grens, et al. (2,4). Hershkowitz and Grens (3) used -60 + 100 mesh coal samples.

C. Chemical Analysis

Separate ASTM ultimate analysis were done by Commercial Testing and Engineering Co., Denver Laboratory (CT and E). The results of these tests were presented in Table III-1.

D. Physical Analysis

The dependence of surface area on particle size was investigated. Samples of -6 + 14 mesh, -14 + 28 mesh, -28 + 60 mesh, -60 + 100 mesh, -100 + 170 mesh, and -170 + 400 mesh were examined and a small dependence of surface area on particle size was observed. Using the surface area of -28 + 60 mesh as a standard, the reduced surface areas (surface area of the sample divided by the average surface area of the -28 + 60 mesh division) ranged from 0.91 to 1.19. Repeated determination were done for each sample size. The average surface areas, the average BET constant, and the reduced surface areas for each of the divisions are reported in Table III-2. These samples were stored under atmospheric conditions in closed containers. Values for -28 + 150 mesh coal are also listed.

The BET constant is believed to be a function of the surface of the sample. The values in Table III-2 indicate of the precision of this quantity since there should be no difference in the respective surfaces.

The pore volume was calculated from the difference between the reciprocals of the particle and actual densities. Actual densities were found by helium displacement and particle densities were found

Table III-1. Analysis of Roland Seam coal proximate analysis.

PROXIMATE ANALYSIS		
	As Received	Dry Basis
% Moisture	23.43-23.83	--
% Ash	10.40-11.49	13.64-15.08
% Volatiles	29.04-35.52	37.93-47.23
% Fixed Carbon	30.16-36.17	39.60-47.23
BTU	8226-8372	10800-10934
% Sulphur	0.70-0.94	0.92-1.23
ULTIMATE ANALYSIS		
	As Received	Dry Basis
% Moisture	23.43-23.83	--
% Carbon	47.02-47.37	61.67-62.19
% Hydrogen	3.79-4.04	4.97-5.30
% Nitrogen	0.73-0.87	0.96-1.13
% Chlorine	0	0
% Sulphur	0.70-0.94	0.92-1.23
% Ash	10.40-11.49	13.64-15.08
% Oxygen (by difference)	11.72-13.55	15.40-17.51

Table III-2. Surface area dependence on particle size.

Particle Size (Tyler Mesh)	Surface Area Dry Basis (m ² /g)	BET Constant	Reduced Surface Area
-6 + 14	95.9	3.6	0.93
-14 + 28	93.5	6.5	0.91
-28 + 60	103	7.0	1.00
-60 + 100	97.8	7.2	0.95
-100 + 170	103	8.9	1.00
-170 + 400	123	8.6	1.19
-28 + 150	99.3	6.1	0.96

by mercury displacement (see Appendix). Since the porisimeter used has a maximum operating pressure of 5000 psig, information was only obtained for pores having an equivalent diameter greater than 0.035 microns. (Equivalent diameter is defined as the diameter corresponding to equilibrium in the Washburn equation.)

The results obtained are an actual density of 1.5 g/cc, a particle density of 1.29 g/cc, and a pore volume of 0.130 cc/g. At 5000 psig only 33% of the pore volume is filled with mercury. No distinguishable difference was detected for samples of -28 + 50 mesh and -50 + 100 mesh sizes. The pore distribution curve for raw coal is shown in Fig. IV-6 for ease of comparison with the curves of the extracted coals.

REFERENCES

- (1) D. Medeiros and E. Petersen, Lawrence Berkeley Laboratory Report LBL-4439 (1975).
- (2) G. P. Dorighi and E. Grens, Lawrence Berkeley Laboratory Report LBL-6335 (1977).
- (3) F. Hershkowitz, Ph. D. Thesis, University of California, Berkeley (1979).
- (4) D. A. Lindsay, M. S. Thesis, University of California, Berkeley (1978).

IV. PHYSICAL PROPERTIES OF EXTRACTED COALS

A. Introduction

Pore size distribution and volumes, actual densities, apparent densities, and surface areas of extracted coals were measured experimentally. As expected, pore volumes increased with yield and the surface area of the samples went through a maximum with progressive extraction. The pore volume and surface area measurements led to interesting conjecture about the nature of the coal surface and changes in the micropore structure as extraction increased. There is reason to believe that a large number of new pores are formed by the removal of material and that the BET constant is a function of the chemical nature of the surface of the adsorbate.

B. Extracted Coal Samples

The extracted coal used in the adsorption studies was obtained from Grens et al. (1,2) wherein detailed extraction procedures and results are presented (see Table IV-1).

Dorigi and Grens used pyridine, ethylenediamine, quinoline, and piperidine as solvents while Lindsay and Grens used pyridine, dipropylamine, and tripropylamine as solvents in the reflux liquid extraction of Roland Seam coal. Yields were varied by conducting the extractions at various temperatures and time of exposure to solvents. However, except where noted, all runs were for 4 hr. The residues (extracted coal samples) were dried at 130°C and 200 mm Hg pressure for 24 hr in a nitrogen purge of 20-25 cc/min. The dried residues were then stored in a desiccator under a vacuum of 100-300 mm Hg nitrogen pressure until needed.

Table IV-1. Extraction conditions and results.

Run No.	Solvent	Extraction Temp. °C	Corrected Extraction Yield (Dry Basis)	Retained Solvent g/g
5	pyridine	250	0.214	0.113
7	dipropylamine	200	0.253	0.144
8	tripropylamine	250	0.163	0.163
10	pyridine	100	0.137	--
11	pyridine	150	0.105	--
12	pyridine	200	0.136	--
13	pyridine	250	0.180	--
14	pyridine	300	0.248	--
15	pyridine	200	0.144	--
16	pyridine	250	0.184	--
18	pyridine (100 hr)	250	0.286	--
19	pyridine	300	0.284	--
22	ethylenediamine	200	0.451	--
23	ethylenediamine	250	0.598	0.154
24	ethylenediamine	150	0.391	--
27	quinoline	350	0.478	--
29	quinoline	300	0.383	--
30	quinoline	250	0.246	--
31	quinoline	200	0.207	--
32	quinoline	250	0.271	0.084
33	piperidine	250	0.340	0.191
34	piperidine	200	0.226	--
36	piperidine	105	0.159	--
37	piperidine (48 hr)	250	0.460	0.204

C. Surface Areas of the Extracted Coals

The extracted coal samples were taken from the desiccator, degassed and the total surface areas were determined by the procedure reported in Chapter II. The BET surface areas were determined by carbon dioxide adsorption at 195°K and by nitrogen adsorption at 77°K (molecular surface areas of 23.4 A² and 16.2 A² were used for carbon dioxide and nitrogen respectively).

The average surface areas obtained for the residues are presented in Table IV-2. The variation of surface area per gram raw coal with extraction yield is shown in Fig. IV-1. Lines are drawn to indicate approximately trends. It appears the surface area depends primarily on the nature of the solvent and the yield. At high yields the pore structure appears to deteriorate (the intersection or pres begins to reduce the surface area).

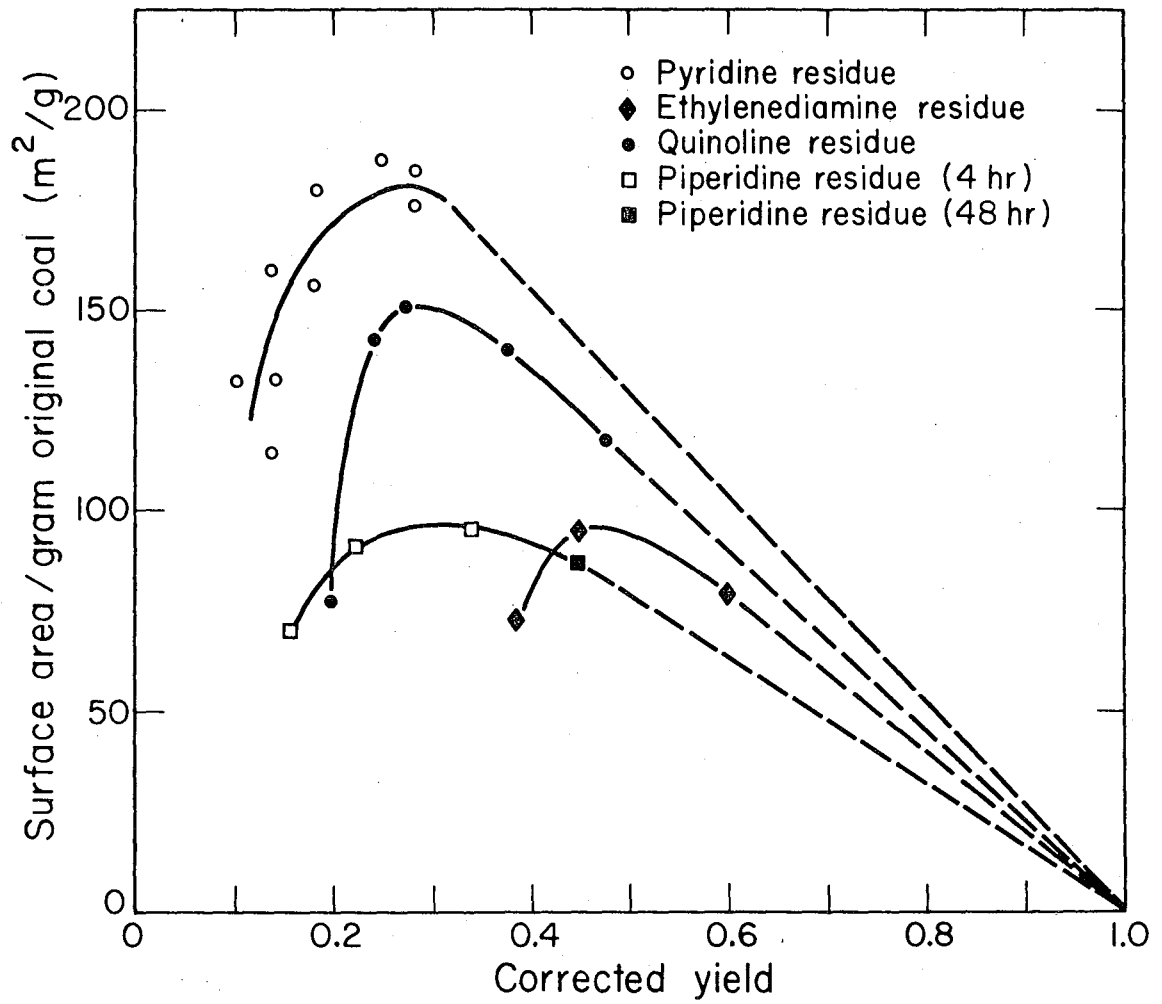
Figure IV-2 shows the relationship between H/C atomic ratio (from Grens et al.) and the BET constant, which is described in Chapter I. This latter constant is the ratio of adsorption of the second layer to the rate of adsorption and first layer. The rate of adsorption of the second layer of adsorbate is assumed constant because carbon dioxide is always adsorbing onto carbon dioxide. The surface of the residue varies with extraction and solvent retainment. The overall H/C ratio was used in Fig. IV-2 to characterize the surface. The appearance of two lines on this figure may stem from the difference in the surface H/C and the overall H/C.

A range of values of the heat of adsorption, 4.4 kcal/mole to 5.6 kcal/mole, was calculated from the definition of the BET constant

Table IV-2. Surface areas of residues.

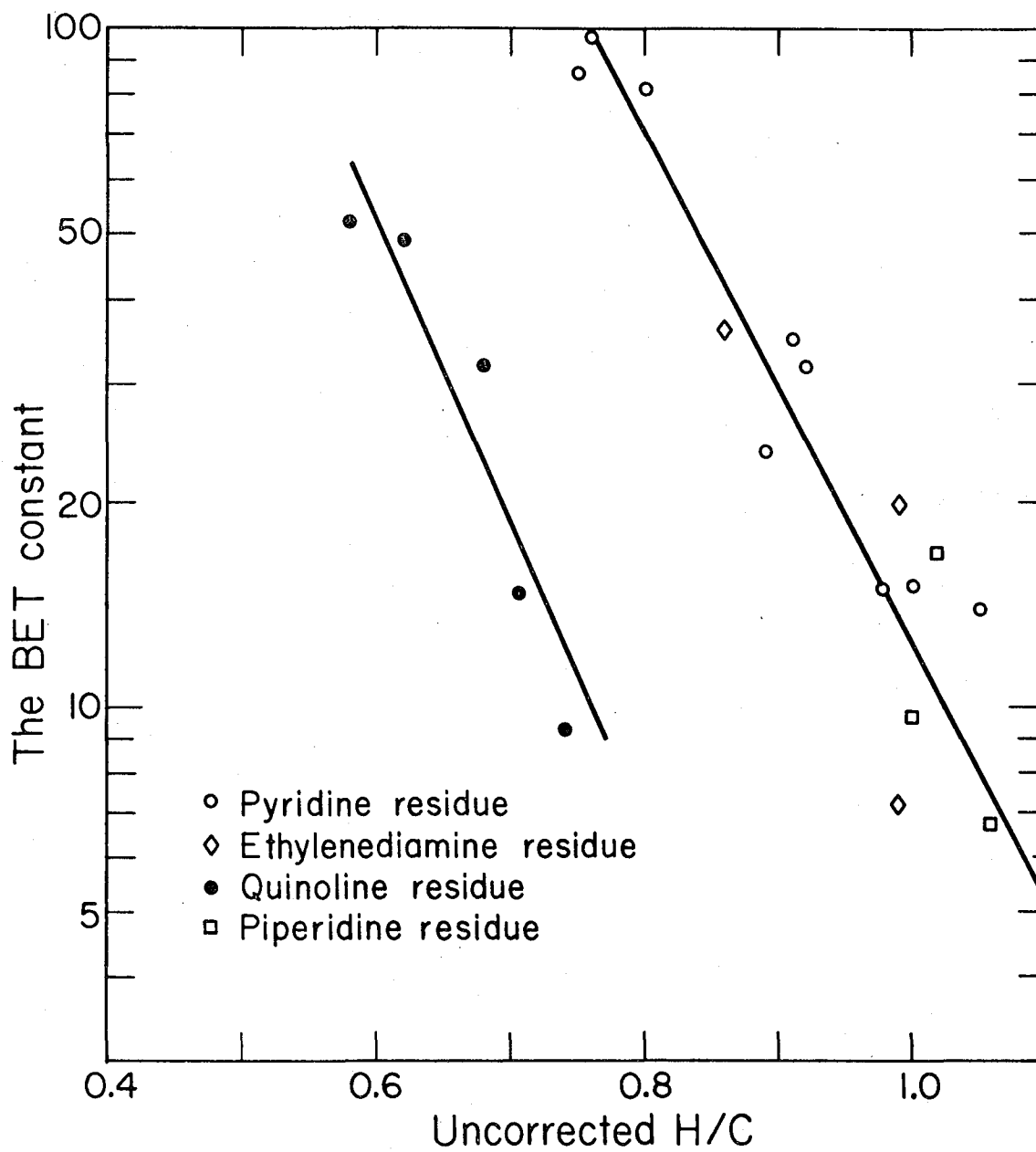
Run No.	CO ₂ Surface Area m ² /g	CO ₂ Surface Area m ² /gram of Raw Coal	CO ₂ BET Constant	N ₂ Surface Area m ² /g
5	247	194	81	10
7	170	127	21	5
8	172	144	19	4
10	134	115	19	-
11	149	133	15	-
12	184	159	15	-
13	190	156	32	-
14	248	189	98	-
15	156	133	24	-
16	220	179	52	-
18	258	184	35	-
19	246	176	86	-
22	176	96	20	-
23	195	79	36	44
24	119	73	7.1	-
27	222	116	52	-
29	226	240	49	-
30	189	143	15	-
31	98	77	9.3	-
32	209	152	27	8
33	144	95	27	8
34	118	91	9.7	-
36	85	71	5.7	-
37	159	88	20	15
Raw Coal	99	99	6.1	1

All surface areas are on a dry basis.



XBL 784-558

Fig. IV-1. Variation of surface area with extraction yield.



XBL 784-557

Fig. IV-2. The effect of H/C on the BET constant of 4 hr extractions.

Table IV-3. Pore volume of extracted coals.

Run No.	Helium Density g/cc	Apparent Density g/cc	Pore Vol. cc/g	Micropore Vol. cc/g	Macropore Vol. cc/g	Calculated Pore Vol. cc/g	Average Pore Diameter A
5	1.62	1.22	0.209	0.110	0.099	0.168	17.8
7	1.51	1.17	0.180	0.078	0.102	0.106	18.4
8	1.45	1.16	0.165	0.077	0.088	0.016	17.9
23	2.15	0.79	0.798	0.228	0.603	0.613	46.8
32	1.75	1.25	0.230	0.101	0.129	0.178	19.3
33	1.57	1.11	0.288	0.093	0.195	0.147	25.8
37	1.83	1.01	0.432	0.171	0.261	0.253	43.0
Raw Coal	1.55	1.29	0.130	0.086	0.042	--	34.6

and the Watson relation for heats of vaporization (3). H/C is a measure of the amount of aromatic material in each residue. As the amount of aromatic material increased, physical adsorption bonds became stronger due to larger intermolecular forces of attraction.

The nitrogen surface areas further support the model of pore structure presented in Chapter III. Since the nitrogen surface areas do not increase as rapidly as the carbon dioxide surface areas, it appears that new pores are being formed as extraction takes place. It is consistent with all data gathered in this study to postulate that the pores in the unextracted coal are reasonably large, with periodic constrictions, some of which are removed during extraction. The number of constrictions removed and the extent of new pores formed appear to depend primarily on yield, solvent molecule size, and the chemical nature of the solvent.

D. Pore Volumes and Distributions

Apparent and actual densities were determined by the procedures described in Chapter II. Pore volumes were determined by the difference in reciprocal densities. Mercury penetration experiments were done on the -50 + 100 mesh section and the -28 + 50 mesh section of the residue. Actual (helium) densities were determined on a well mixed sample of the residue. It was assumed that densities were not a function of particle size. Repeated runs of the two density experiments were done for selected samples and their average values are reported in Table IV-3. They indicate the residue approaches the structure of graphite with progressive extraction.

Micropores were defined as those with equivalent diameters less than 350 A because the porosimeter used could only penetrate the remaining pores, the macropores. Assuming all of the surface area is in the micropores the average diameter of the micropores decreases with all of the selected samples except for ethylenediamine (run 23) and the 48 hr piperidine (run 37) residues. This is consistent only if a large number of new pores are formed.

In Fig. IV-3, total pore volumes are plotted against yield, which is corrected for solvent retention by a nitrogen balance. By knowing the amount of retained solvent the pore volume after extraction can be predicted. To do this, the density of the removed material was assumed to be the same as raw coal. Pore volumes were then calculated by:

$$V_{pac1} = (V_0 + Y_C/\rho - V_r)/(1 - Y_C + m_S)$$

where:

V_{pac1} = calculated pore volume, cc/g residue.

V_0 = pore volume of raw coal, cc/g.

Y_C = yield corrected for solvent retainment.

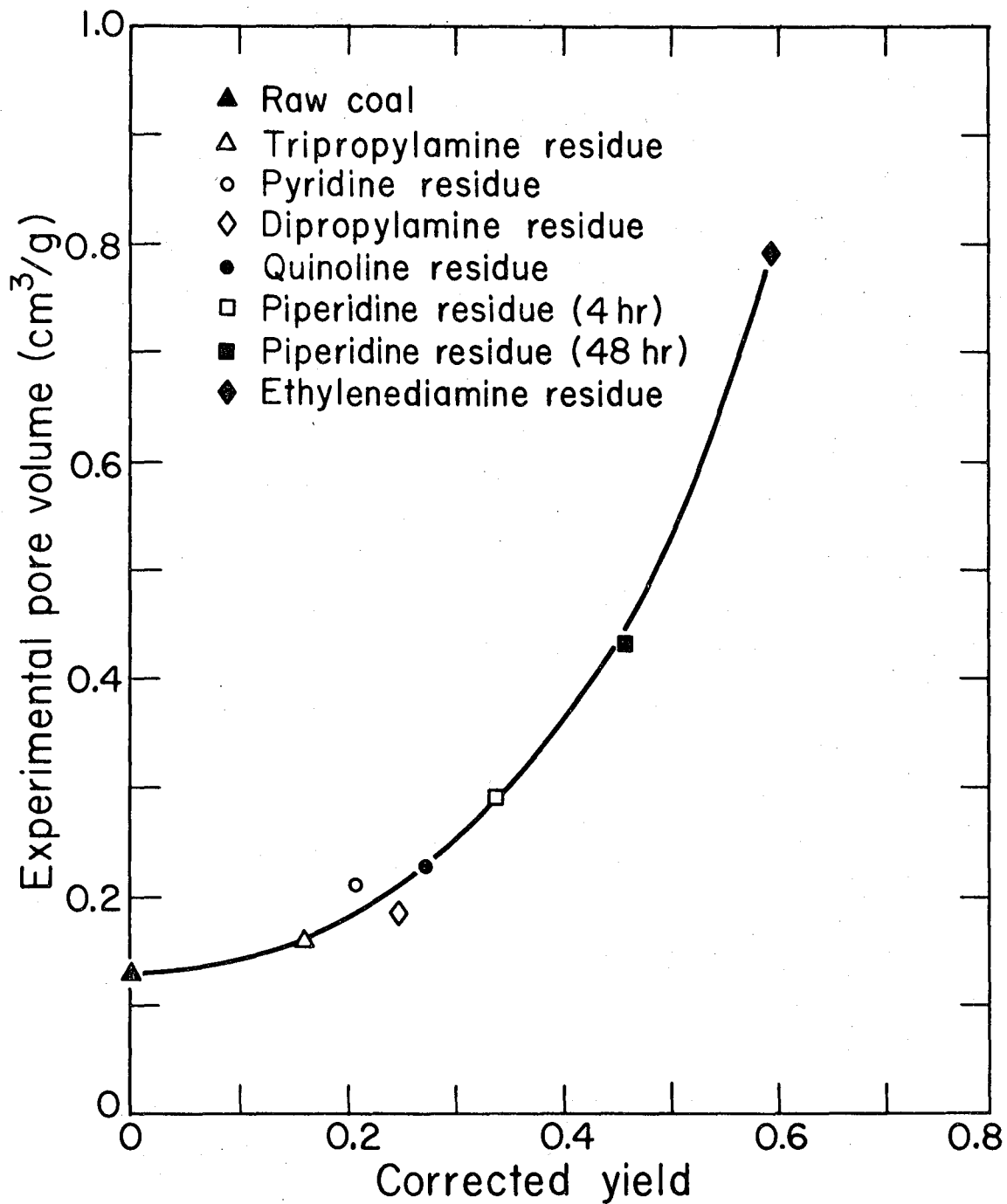
V_r = volume of solvent retained, cc/g residue

ρ = actual density of raw coal, g/cc.

m_S = mass of solvent retained, gram of solvent/gram of residue,

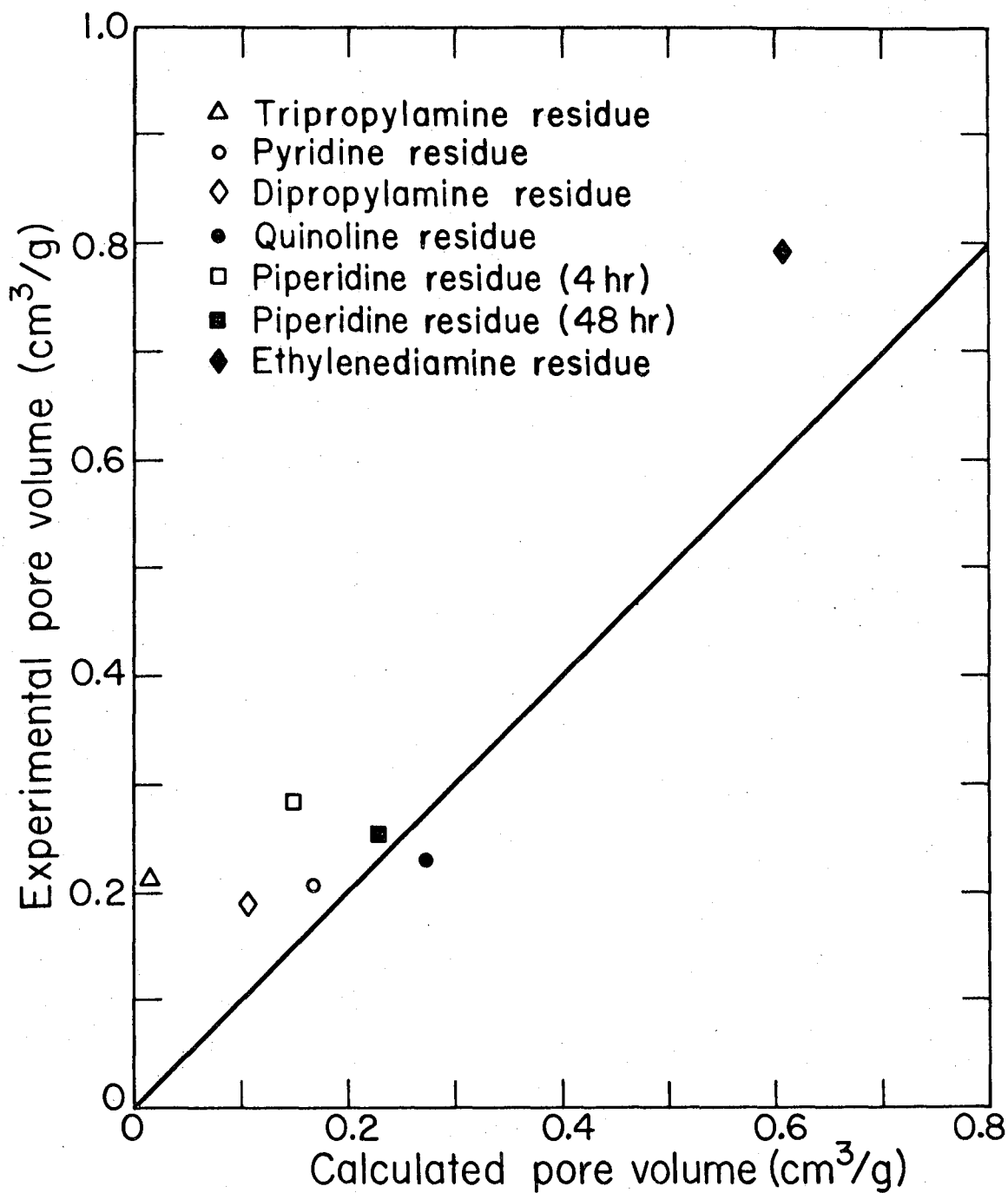
listed in Table IV-1 for the selected samples.

Figure IV-4 has the experimental pore volumes plotted against the calculated pore volume. It shows that the solvents do remove the lighter molecules and leave the macromolecules.



XBL 784-554

Fig. IV-3. Pore volume's dependence on yield.



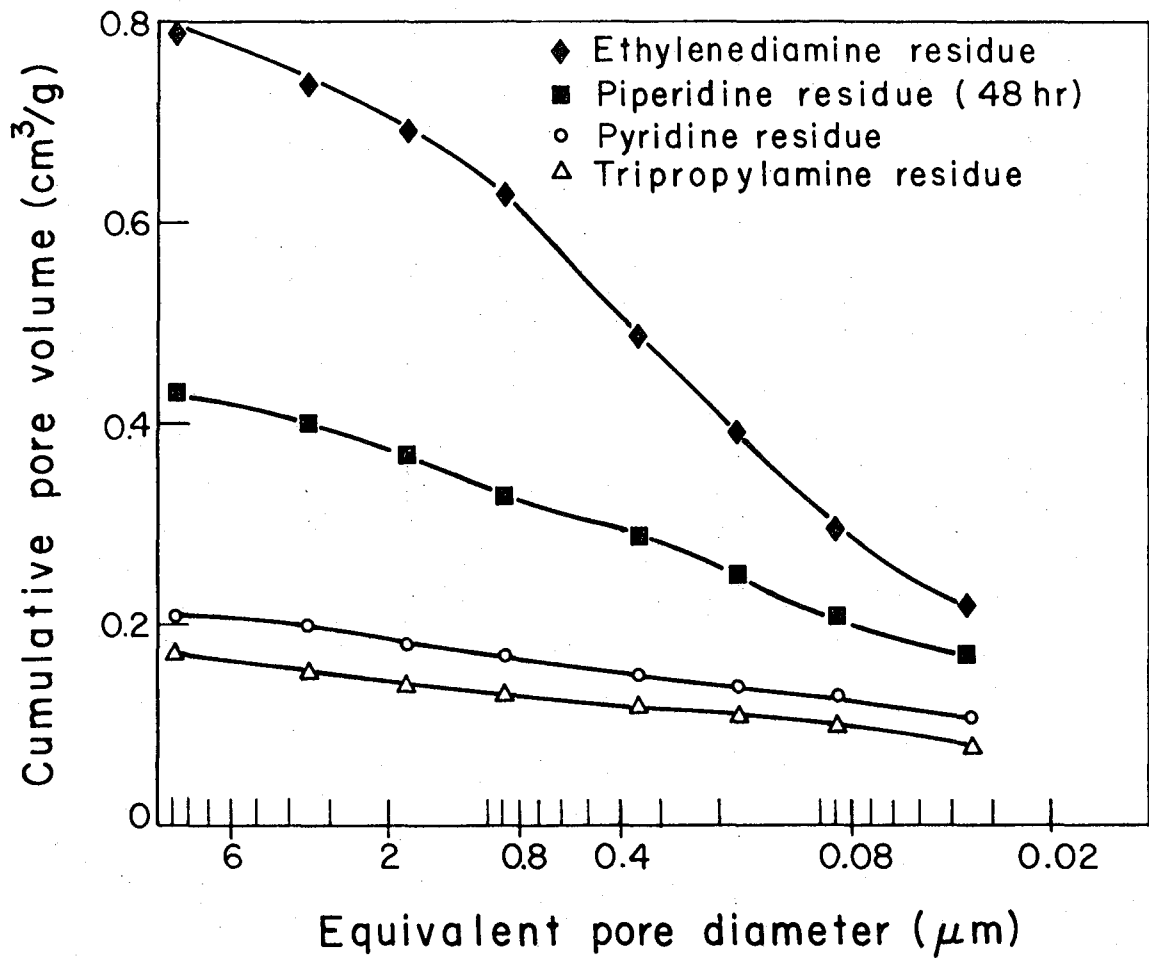
XBL 784-553

Fig. IV-4. Experimental pore volume vs calculated pore volume.

Pore distribution curves for the selected samples are shown in Figs. IV-5 and IV-6. They indicate that for each solvent the pore sizes measured extraction is independent of the pore size.

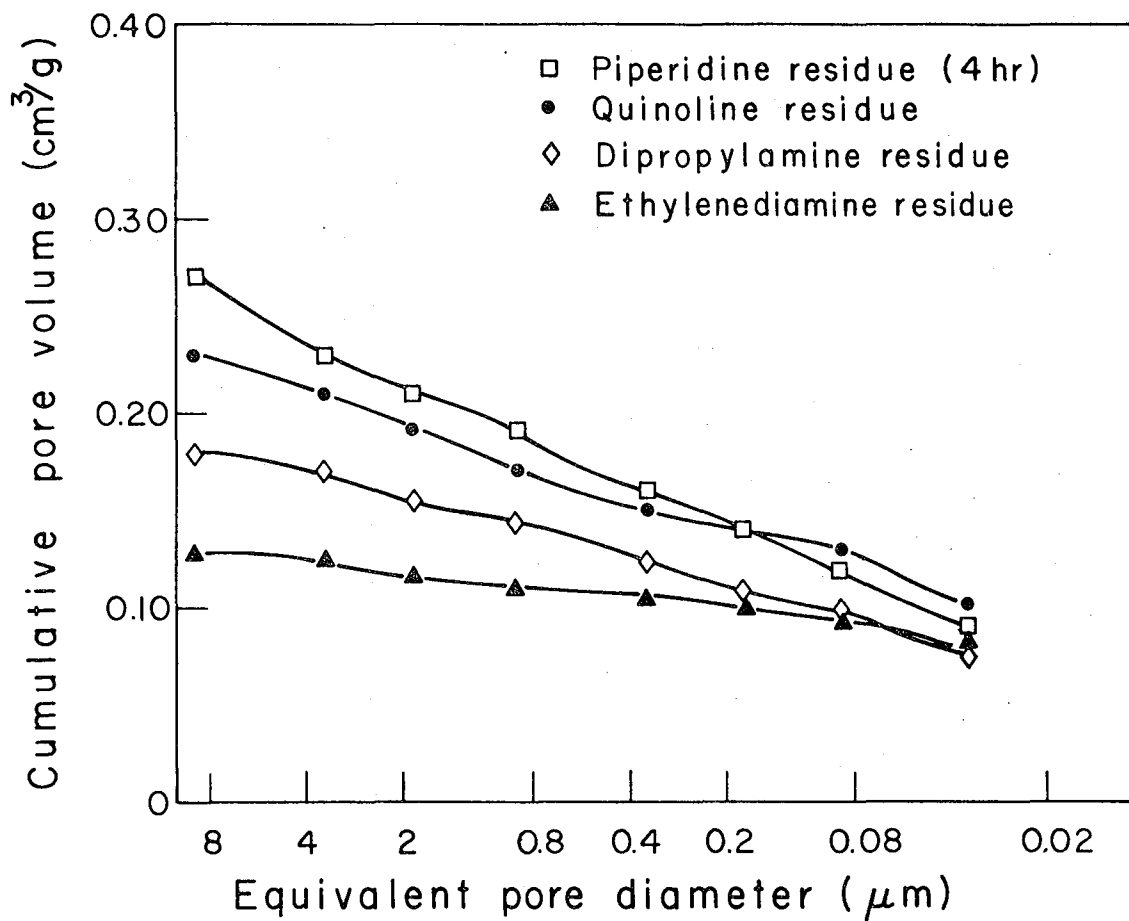
Samples were chosen for study on the basis of their high yield and similar extraction conditions.

The pore-volume and surface area measurements on raw and extracted coals strongly suggest that Roland Seam coal has two pore systems (4). The macropores have large volume, small surface area, and no mass-transfer limitations; while the micropores have small volume, large surface area, and some mass transfer limitations. The micropores appear to have small constrictions of the order of 4 A that inhibit the flow of solvent into the micropores. This model of the pore structure accounts for all of the known physical characteristics of raw and extracted Roland Seam coal. No attempt was made to determine the magnitude of swelling of coal by the solvent or by thermal expansion during extraction, although both are believed to be small. An attempt was made to determine qualitatively the general shape of the pore structure from the changes in the pore volume and the surface area, but due to the complexity of the structure and to solvent entrainment the results were inconclusive.



XBL 784-555

Fig. IV-5 Pore distribution of extracted coals.



XBL 784-556

Fig. IV-6. Pore distribution of extracted coals.

REFERENCES

- (1) G. P. Dorighi and E. A. Grens, Lawrence Berkeley Laboratory Report LBL-6335 (1977).
- (2) D. A. Lindsay, M. S. Thesis, University of California, Berkeley (1978).
- (3) R. C. Reid, J. M. Prausnitz and T. K. Sherwood, The Properties of Gases and Liquids, 210 (1977).
- (4) P. Zwietering and D. W. Van Krevelen, Fuel 33, 331 (1954).

V. SURFACE AREA VARIATION OF REACTED ROLAND SEAM COAL

The samples for this portion of the research were obtained from Hershkowitz and Grens (1), who give detailed reaction procedures and results. These surface areas, measured by carbon dioxide adsorption at 195°K, indicate that hydrogenation increased the selectivity of the extraction solvents.

The coal samples (-28 + 100 mesh) were reacted with molten zinc chloride and an organic solvent (see Table V-1). The reactions were all carried out in a reaction vessel at 250°C for 1 hr under either a hydrogen or solvent atmosphere. After reaction, the melt treated coal (MTC) was extracted with benzene and pyridine, respectively, in an atmospheric boiling Soxhlet.

The surface areas of the reacted coal samples were measured by the procedures reported in Chapter II, and are reported in Table V-2 on a dry basis. The RC refers to the residue of the treated coal after extraction.

Generally the surface areas are larger for extracted residues with hydrogenation than for those without hydrogenation for the same yield, indicating a higher surface roughness that is due to a preferentially increased solubility of the coal hydrogenation. The surface areas of MTC show that pretreatment with zinc chloride under the proper conditions removes some material, and does not physically hinder the solvent extraction process. Because of the large variation in the reaction conditions, more detailed conclusions are impractical.

REFERENCE

- (1) F. Hershkowitz, Ph. D. Thesis, Univ. of California, Berkeley (1979).

Table V-1. Conditions of selective hydrogenation.

Run No.	Amt. of Coal Grams	Amt. of ZnCl ₂ Grams	Amt. of H ₂ psig	Amt. of Solvent Grams
1	50	--	--	--
2	50	300	500	--
3	50	300	500	--
4	50	300	--	--
5	50	300	--	50 (tetralin)
6	50	300	500	50 (tetralin)
7	50	300	500	50 (tetralin)
8	25	25	500	150 (tetralin)
9	50	300	500	50 (isopropanol)
10	50	300	500	50 (t-butanol)

Table V-2. Surface area variations of reacted coals.

Run No.	Extraction Yield	Surface Area of MTC mm/g	BET Constant of MTC	Surface Area of RC mm/g	BET Constant of RC
1	0.101	--	--	145	16
2	0.163	180	29	268	97
3	0.163	170	9.4	254	53
4	0.115	215	9.9	283	47
5	0.604	101	5.3	309	67
6	0.677	106	2.2	245	52
7	0.687	101	3.3	236	95
8	0.298	140	30	231	66
9	0.709	89.2	8.7	216	27
10	0.292	156	23	260	88

VI. CONCLUSIONS AND SUGGESTIONS FOR FUTURE WORK

A. Conclusions

Carbon dioxide and nitrogen adsorption on raw coal yield vastly different surface areas. This study, the work of Medeiros (1) on molecular sieves, and the size of the average micropore diameter suggest that the pores have large equivalent diameters with random constrictions. Decreases in the average pore diameter and the small, but significant increases in the nitrogen surface areas, due to extraction, lead to the conclusions that new pores are being formed while old pores are being enlarged. The lack of major inflection points in the pore distribution curves and the generation of new pores indicate that the original pore structure is not a limiting factor in the liquefaction process.

The variation of surface area with yield for the same solvent shows a deterioration in the pore structure at high yields. If this was not the case, the plot of surface areas per gram raw coal would not go through a maximum. For pyridine, quinoline, and piperidine, deterioration begins at about 30% yield, whereas for ethylenediamine it starts at about 45% yield. The difference is probably due to size effects of the solvent molecules.

Comparing the calculated pore volumes to the experimental pore volumes confirms the theory of preferential removal of solid material by molecular size. Only in the case of quinoline does the comparison fail, which suggests that quinoline, the highest molecular weight material used as a solvent, removes a significantly higher proportion of the heavier molecules than the other solvents do.

Hydrogenation of the coal before extraction produced higher surface areas for the same yield. The increased selectivity of the solvents is shown by the increased surface roughness.

The surface of the residue apparently becomes more favorable for carbon dioxide adsorption with increasing extraction. This is exemplified by the increase in the BET constant with decreasing H/C.

B. Suggestions

Valuable information could be obtained by doing detailed micropore distribution studies. The prevailing method is by nitrogen or carbon dioxide condensation and can give distribution curves of pores larger than 12 Å in diameter (2). This information should confirm the conclusions of this study.

The effect of swelling of coal due to solvent contact was assumed to be insignificant in this study. This should be investigated. If it is substantial, it could explain why solvent molecules can enter the constrictions in the pores.

REFERENCES

- (1) D. Medeiros and E. Petersen, Lawrence Berkeley Laboratory Report LBL-4439 (1975).
- (2) H. Gan, S. P. Nandi and P. L. Walker, Fuel 51, 272 (1972).

ACKNOWLEDGEMENT

This work was done under the auspices of the U. S. Department of Energy through the Lawrence Berkeley Laboratory, Berkeley, California.

APPENDIX A. A METHOD OF DETERMINING PARTICLE DENSITIES OF SPHERIODS

Particle density is defined as the reciprocal of the sum of the specific volume and pore volume. Using a mercury porosimeter, particle densities are easily measured.

By a summation of forces, the pressure necessary to fill interparticle voids can be evaluated. At equilibrium, the force due to external pressure is equal to the force due to surface tension (1).

$$\begin{aligned} AP &= -L\sigma \\ A &= (\sqrt{3} - \pi/2) R^2 \\ L &= b\pi R \cos \alpha \end{aligned} \quad (A-1)$$

where:

R = radius of spheriod

b = coefficient of surface roughness

$b = \frac{\text{actual linear distance of contact}}{\text{idealized linear distance of contact}}$

α = wetting angle, 140°.

P = pressure

σ = surface tension, 484 dynes/cm.

By rearrangement

$$P = -\pi b \sigma \cos \alpha / (R(\sqrt{3} - \pi/2)) \quad (A-2)$$

This applies to porous spheroids of any size, as long as the size range of the samples is sufficiently narrow. It is recommended that the variation in particle size be such that the pressure that will penetrate the largest pores of the largest particles is twice that which will fill an interparticle void created by the smallest particles.

The minimum pressure that will fill the largest pores of the largest particle is determined by a force balance over the pore opening using an appropriate model for the shape of the pore (cylinders, slots, etc.) (2) and a correlation between the pore size and particle size. By using an scanning electron microscope, the correlation and model can be determined to within engineering accuracy.

Walker et al. (3) reported that it took about 20 psia to fill interparticle voids of Buck Mountain coal (-40 + 70 U. S. mesh). By using the radius of 70 mesh spheroids, b is calculated to be about 2, in agreement with Wheeler (4).

Experiments using glass beads were done to check the accuracy of Eq. (A-2). The following are our results.

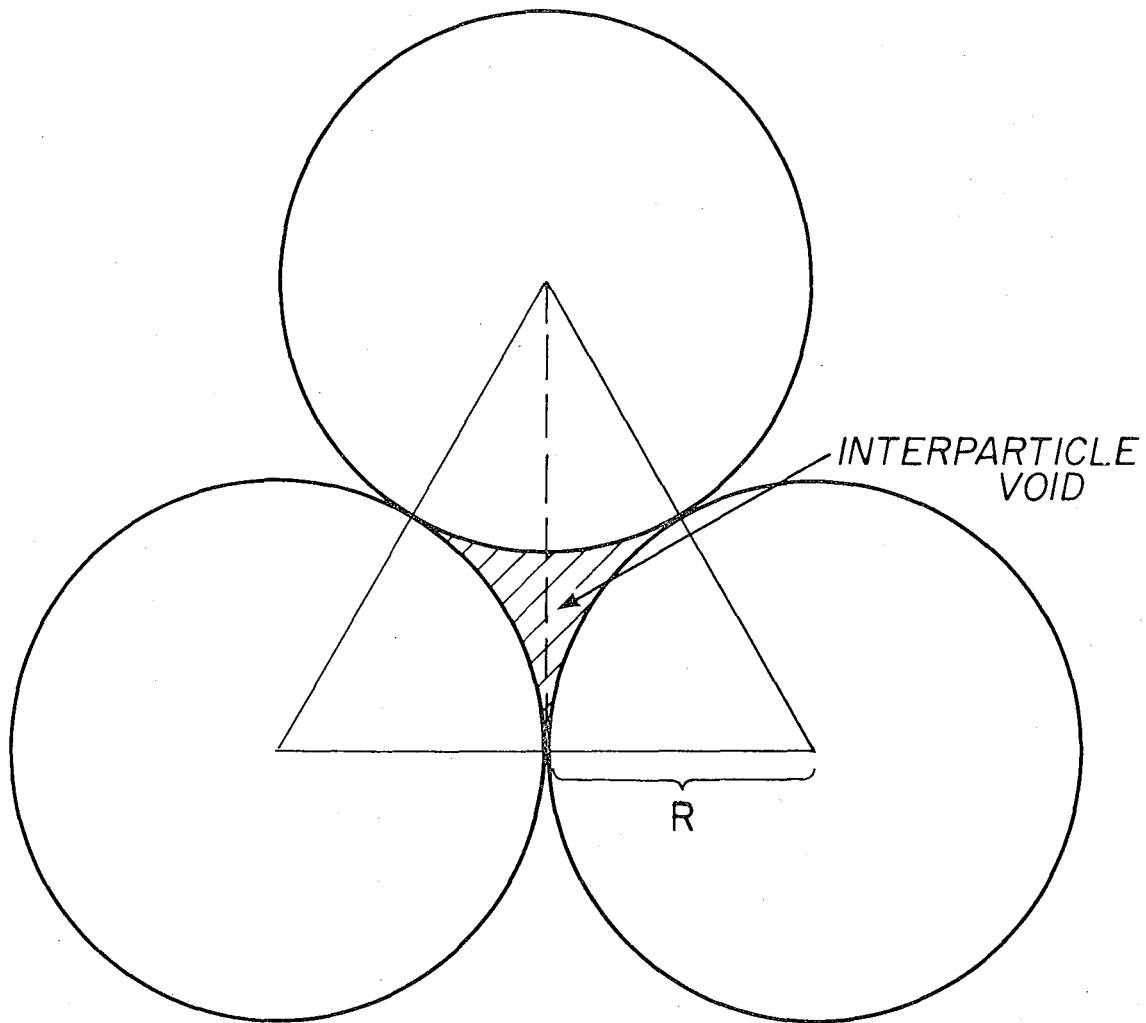
Sample Size Radius (mm)	Theoretical Pressure	Measured Density at Theoretical Pressure	Measured Density at 5000 psig
2.25	0.93	3.00	3.00
0.75	2.79	2.50	2.52
0.15-0.30	14.0	2.52	2.52
0.075-0.15	27.9	2.52	2.53
0.053-0.075	39.5	2.50	2.51
0.037-0.053	56.6	2.52	2.53

The maximum error is 0.8% in the above table. The agreement between experiment and theory is sufficient to validate the theory.

This theory is needed only for porous materials having large macropores. For these materials, it is quite conceivable that the largest pores are being filled when interparticle voids are still empty. For material not having such large macropores it is readily seen during the penetration experiment when the interparticle voids are filled when doing a mercury penetration experiment.

REFERENCES

- (1) E. W. Washburn, Proc. Natl. Acad. Sci. 7, 115 (1921).
- (2) R. L. Bond, Nature 178, 104 (1956).
- (3) H. Gan, S. P. Nandi and P. L. Walker, Fuel 51, 272 (1972).
- (4) A. Sheeler, AAAS Gordon Conference on Catalysis Report NO. S-9829 (1945).



XBL 784-559

Fig. A-1. An interparticle void.

This report was done with support from the United States Energy Research and Development Administration. Any conclusions or opinions expressed in this report represent solely those of the author(s) and not necessarily those of The Regents of the University of California, the Lawrence Berkeley Laboratory or the United States Energy Research and Development Administration.